

Photoelectron spectroscopy of mass-selected metal cluster anions.

I. Cu_n^- , $n = 1-10$

Doreen G. Leopold,^{a)} Joe Ho, and W. C. Lineberger

*Department of Chemistry, University of Colorado and Joint Institute for Laboratory Astrophysics,
University of Colorado and National Bureau of Standards, Boulder, Colorado 80309*

(Received 23 September 1986; accepted 31 October 1986)

Negative ion photoelectron spectra of Cu_n^- ($n = 1-10$) are reported for the 0–2.4 eV region at an instrumental resolution of 10 meV. The cluster anions were prepared in a flowing afterglow ion source incorporating a cold cathode dc discharge. This very simple source provides a convenient, general method to prepare continuous beams of near-thermal metal cluster ions at intensities (up to 10^{-11} A) sufficient for spectroscopic or chemical studies. Photoelectron spectra of the copper cluster anions yield measurements for vertical electron binding energies and adiabatic electron affinities as a function of cluster size. The overall trend observed is well described by the classical spherical drop electrostatic model. In addition, quantum effects are apparent in the higher electron affinities generally observed for clusters containing odd numbers of atoms. Excited electronic states in the photoelectron spectra show that the transition energy in the neutral molecule decreases rapidly with cluster size. Vibrational structure resolved in the Cu_2^- spectrum yields measurements for the vibrational frequency ($210 \pm 15 \text{ cm}^{-1}$), bond length ($2.345 \pm 0.010 \text{ \AA}$), dissociation energy ($1.57 \pm 0.06 \text{ eV}$), and vibrational temperature ($450 \pm 50 \text{ K}$) of the anion.

I. INTRODUCTION

The past decade has witnessed a virtual explosion of interest in the spectroscopic, structural, and chemical properties of small metal particles.^{1,2} A major goal of this work has been to characterize the evolution from the molecular to the bulk metallic state, and ultimately to forge a link between the now disparate conceptual frameworks of molecular quantum chemistry and surface science. Thus, much effort has been directed toward examining the dependence of well-defined electronic structure properties on the number of atoms comprising a cluster. On the theoretical front, there is now a large body of work concerning metal cluster electron affinities³⁻¹¹ and ionization potentials³⁻²⁴ and their approach toward the bulk work function with increasing cluster size. In addition, numerous calculations have investigated the energy gap between the highest occupied and lowest unoccupied molecular orbitals as a function of cluster size and the development of bulk electronic band structure,^{6-8,18,21-23,25-29} defining features of the metallic state.

In contrast, relatively few experimental data are available to test these models of the size dependence of metal cluster electronic structure. This scarcity is due in large part to the difficulty of extracting information concerning particles of definite size from samples containing cluster distributions. Until quite recently, the only particle-specific data available for an electronic property as a function of metal cluster size were ionization potential measurements for alkali clusters.³⁰⁻³³ Just within the past four years, dramatic improvements in metal cluster generation and laser mass spectrometric techniques have enabled the extension of such measurements to transition metal clusters. Ionization poten-

tials have now been obtained from photoionization threshold experiments for Nb,³⁴ Fe,³⁵ Ni,³⁶ and Cu³⁷ clusters of up to about 25 atoms.

Experimental data for electron affinities and other aspects of metal cluster electronic structure have been scarcer yet. Smalley and co-workers³⁸ have investigated laser fluence dependences of relative cross sections for photo-detachment from Cu_n^- ($7 \leq n \leq 30$) anions to obtain estimates of upper and lower bounds for the neutral cluster electron affinities. A recent investigation of autoionizing inner-shell transitions in mercury clusters by Brechignac *et al.*³⁹ provides the only direct experimental measurement of the development of electronic band structure in metal clusters of definite size. To our knowledge, no other gas phase spectroscopic data have been reported for bare transition metal clusters containing more than three atoms.

Laser photoelectron spectroscopy of negative ions⁴⁰ potentially provides a very powerful technique for investigating the electronic structures of size-selected metal clusters. The measurement of photoelectron kinetic energies yields information concerning Franck-Condon factors for electron attachment, enabling the precise determination of adiabatic electron affinities. In addition, the experiment provides a direct probe of the low-lying excited electronic states of the neutral cluster. Photoelectron spectra have thus far been reported for Fe_2^- ,⁴¹ Co_2^- ,⁴¹ and Re_2^- .⁴² However, extension of these studies to larger metal clusters has been impeded by the lack of a general, continuous source for the production of metal cluster anions at the low temperatures required for detailed spectroscopic characterization.

In this paper, we describe a simple method for producing continuous beams of transition metal cluster anions near room temperature. This technique employs a cold cathode dc discharge in a flowing afterglow⁴³ ion source, enabling the convenient preparation of mass-selected cluster anion beams

^{a)} Present address: Department of Chemistry, University of Minnesota, Minneapolis, MN 55455.

at intensities (10^{-13} – 10^{-11} A) adequate for spectroscopic analysis.

We have used this source to measure the negative ion photoelectron spectra of Cu_n^- , $n = 1$ – 10 . These systems have been chosen as our initial targets in view of the relative theoretical tractability of clusters of closed d -shell, "alkali-like" Cu atoms. As a result of numerous experimental^{44–49} and theoretical^{4,13,16,18,22,27,50–54} studies, Cu_3 is now undoubtedly the best understood polyatomic transition metal molecule. Although a large body of theoretical work has also been devoted to copper clusters containing more than three atoms,^{16(a),18,22,23,26,27,29,55} and some matrix data are available,^{44,56} no gas phase spectroscopic studies have been reported to date. The present investigation provides new information concerning the adiabatic electron affinities and vertical detachment energies of small copper clusters, and the cluster size dependence of the energy gap between the ground and the lowest photoelectron-allowed excited electronic states in these model systems.

II. EXPERIMENTAL METHOD

A complete description of the negative ion photoelectron spectrometer has previously appeared.^{57,58} Briefly, anions are prepared in a flowing afterglow ion source, gently extracted into the low pressure region of the apparatus, and mass selected. The beam of selected anions is then decelerated and crossed by the intracavity beam of a cw argon ion laser tipped at the "magic angle" yielding photodetachment signal intensities proportional to average photodetachment cross sections.⁵⁹ A small fraction of the photodetached electrons are energy analyzed at a resolution of ~ 10 meV (80 cm^{-1}) by a hemispherical electrostatic monochromator, and detected by a two-dimensional position sensitive detector. In the present study, the absolute electron kinetic energy scale was calibrated against the known electron affinities of W ($0.815 \pm 0.002 \text{ eV}$ ⁶⁰) and O.⁶¹ Spectra were also corrected for an energy scale compression factor⁵⁸ of 1.6%, determined from atomic fine structure splittings⁶² in the W^- photoelectron spectrum.

Copper cluster anions were prepared in a flowing afterglow ion source identical to the one previously described⁵⁷ except for the substitution of a cold cathode dc discharge for the former ionizer. In the discharge source, metal atoms and clusters are sputtered from the cathode by bombardment with Ar^+ or other cations. Further interactions with the dense plasma yield metal anions (and undetected cations), which can form larger clusters by ion–molecule reactions during their 10^{-2} s residence time in the flow tube. The very simple design employed in the present experiment is illustrated in Fig. 1. The cathode consists of a 1 in. long tube of 1/4 in. o.d. OFHC copper positioned on the axis of the 1.8 in. i.d. flow tube. Mechanical support and electrical contact are provided by a 1/8 in. diam OFHC copper wire passing through the cathode. The wire is insulated with alumina tubing secured to the vacuum flange by a 1/4 in. O-ring fitting and epoxied at the end to form a vacuum seal. The stainless steel flow tube serves as the (anisotropic) anode, and the fast ($\sim 60 \text{ STP cm}^3 \text{ s}^{-1}$) gas flow provides directionality. To minimize heating, the external portions of the 30–50 cm long

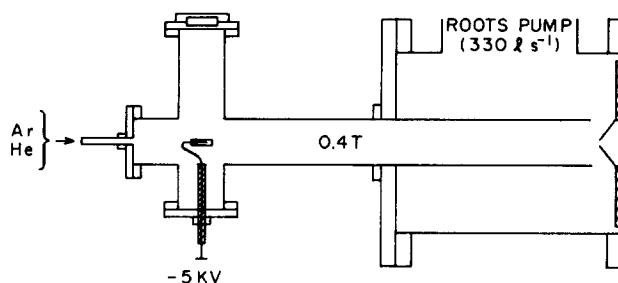


FIG. 1. Cross-sectional scale drawing of the flowing afterglow ion source equipped with a cold cathode dc discharge for the production of metal cluster ions. A tube and/or wire of the material to be sputtered is negatively biased at 4–5 KV with respect to the grounded stainless steel flow tube. The discharge typically draws 30 mA and is operated with a 6:1 He:Ar mixture at 0.4 Torr. The fast ($\sim 60 \text{ STP cm}^3 \text{ s}^{-1}$) gas flow directs the sputtered material down the 30–50 cm long flow tube, where collisions afford further cluster growth and relaxation of internal degrees of freedom. The window is used for viewing the discharge during operation. Ion lensing following the 1 mm diam sampling aperture remains as described in Ref. 57.

flow tube and cathode assembly are wrapped with water-cooling coils.

Gas composition, pressure, and discharge voltages used in these experiments were adjusted to optimize copper cluster anion yields. The cathode was negatively biased at 4–5 KV with respect to the grounded flow tube, producing a discharge current of about 30 mA in a mixture of 10%–20% Ar in He at 0.4 Torr. Bare copper cluster production was found to be very sensitive to oxygen impurities. To minimize contamination, the helium was purified by passage through a coiled column of liquid nitrogen cooled molecular sieves and UHP Ar was used. In addition, the OFHC copper cathode was electrochemically cleaned prior to use.

Operation of the discharge source was, in general, remarkably convenient. Once favorable operating conditions were established, the source routinely ran for days at a time with minimal adjustment. Examination of the used cathode showed uniform sputtering of its outer surface and of the supporting wire. In the case of copper, a loss of 1 g of cathode material was measured following about 20 h of use.

III. RESULTS

A. Metal cluster anion production

Figure 2 displays a typical mass spectrum of copper clusters prepared in the cold cathode discharge ion source. Anion abundances increase with increasing cluster size, from 1 pA for Cu^- to 10 pA (6×10^7 ions/s) for Cu_5^- . Intensities of higher clusters display a reproducible maximum at Cu_7^- . Anions of more than ten atoms are doubtless produced but are difficult to detect due to the reduced resolution of our Wien velocity filter at higher masses. Between Cu_4^- and Cu_8^- , our mass spectrum also displays the odd > even intensity alternation observed in previous mass spectrometric studies of Cu_n^- ,³⁸ Ag_n^- ,^{63,64} Cu_n^+ ,^{37,63} and Ag_n^+ .⁶³

Successful operation of the metal cluster anion source was not limited to copper, a particularly efficient target⁶⁵ for Ar^+ sputtering. In fact, use of a nickel electrode yielded larger ion beam intensities than were observed for copper under identical flow tube conditions. A nickel discharge at

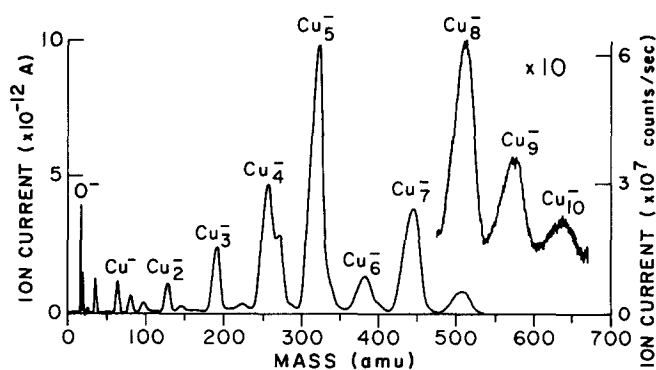


FIG. 2. Mass spectrum of Cu_n^- anions prepared in a cold cathode dc discharge source. The cathode was an OFHC copper tube (1 in. long, 1/4 in. o.d.) positioned 50 cm from the sampling aperture. Unlabelled peaks to the right of Cu_n^- are copper oxides; those at low mass are F^- and Cl^- impurities.

– 4 KV and 30 mA in a 30 cm long flow tube at 0.4 Torr (7:1 He:Ar at a total flow rate of $\sim 60 \text{ STP cm}^3 \text{ s}^{-1}$) produced detectable cluster anions up to Ni_{10}^- , with a maximum of 50 pA at Ni_4^- . The mass spectrum of Ni_n^- did not show the odd/even intensity alternation observed for copper. Rather, a smoothly varying distribution of ion intensities was observed with the notable exception of a near total absence of Ni_2^- .

Tungsten, one of the most difficult materials to sputter,⁶⁵ also gave abundant products. Use of a tungsten wire as the cathode under discharge conditions similar to those described above routinely produced W^- in intensities adequate for calibration purposes. The major molecular product anions were WO_3^- (30 pA) and W_2O_3^- (10 pA), probably arising from tungsten oxide cathode impurities. Use of a platinum electrode yielded Pt_n^- and Pt_nO_m^- signals of up to 30 pA for $n = 1-3$, an artificial limit imposed by the high-mass cutoff of our mass analyzer. Thus, the cold cathode discharge flowing afterglow source provides a general yet remarkably simple method to produce continuous beams of metal cluster anions with intensities on the order of picoamps.

Heteronuclear anions were readily prepared by the addition of reactant gases to the He/Ar buffer. For example, PtN^- , $\text{Ni}(\text{CO})_2^-$, and CuF^- were synthesized by addition of N_2 , CO, or fluorocarbon gases. Replacement of Ar with O_2 gave nearly complete conversion of the bare copper clusters to copper oxides. These examples illustrate the potential use of this source for the synthesis of partially ligated species, and for chemical studies of metal cluster anions.

Vibrational temperatures of anions prepared in this source can be estimated from hot band intensities in the photoelectron spectra. For example, a temperature of $500 \pm 50 \text{ K}$ was determined for the CuF^- $480 \pm 20 \text{ cm}^{-1}$ vibration. The spectrum of Cu_2^- , discussed in the following section, gave essentially the same result ($450 \pm 50 \text{ K}$) for the 210 cm^{-1} vibration. Since rotational relaxation is, in general, more efficient than vibrational relaxation in a flowing afterglow source,^{57,66,67} as in a supersonic expansion,⁶⁸ an upper limit of 500 K can be deduced for the rotational temperature. A more likely value of $\sim 300 \text{ K}$ is given by the temperature

usually observed for our flowing afterglow when an electron gun,^{57,69} or a microwave discharge^{41,70} is used as the ion source.

Electronic state population distributions are not expected to attain thermal equilibrium by collisional relaxation in the afterglow, and thus an electronic temperature cannot be estimated. However, we note that the photoelectron spectra of the copper cluster anions discussed in the next section showed possible evidence for significant electronic excitation only in the case of Cu_3^- . Even in this case, the possible electronic hot band was more than two orders of magnitude weaker than the ground state transition. Thus, it appears that the copper cluster anions sampled from the flow tube are virtually entirely in their ground electronic states.

B. Photoelectron spectra of copper cluster anions

1. General observations

Figure 3 shows the negative ion photoelectron spectra of Cu_n^- , $n = 1-10$. The data were obtained at excitation energies of 2.540 (488 nm) or 2.707 eV (458 nm); the five times more intense 488 nm Ar^+ laser line was used to collect all data in the 0–2.2 eV region. For convenient comparison of

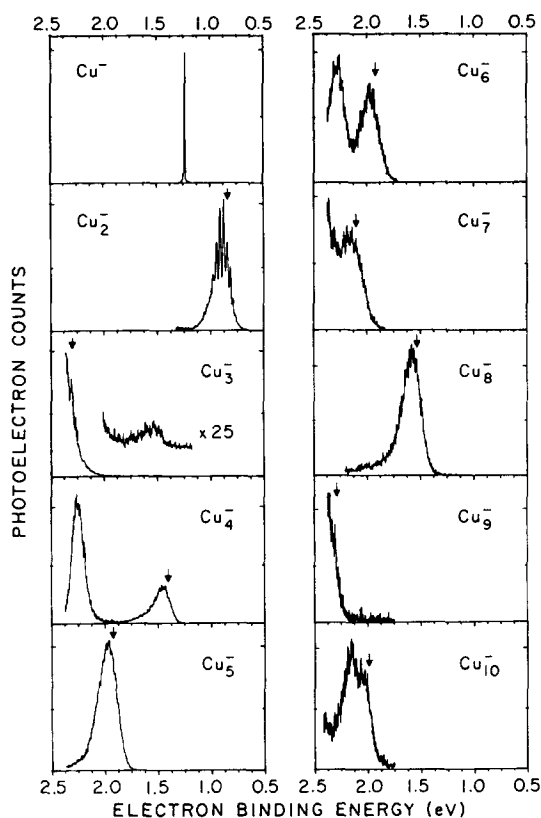


FIG. 3. Photoelectron spectra of Cu_n^- obtained at 488 (2.540 eV) or 458 nm (2.707 eV) at an instrumental resolution of $\sim 10 \text{ meV}$. Full scale photoelectron counts range from 3000 (Cu_2^-) to 20 (Cu_5^-). Vibrational structure is resolved for Cu_2^- only. Arrows indicate positions of adiabatic electron affinities determined as described in the text; for Cu_3^- and Cu_5^- arrows show minimum values. Transitions to excited electronic states of the neutral Cu_4 , Cu_6 , Cu_7 , and Cu_{10} clusters are also observed. The weak band shown on an expanded scale in the Cu_3^- spectrum is evidently due to an excited electronic state of the anion. Scans over the entire 0–2.4 eV range for Cu_{7-10}^- (not shown) revealed no additional features.

spectra taken at different wavelengths, the data are plotted as a function of electron binding energy, equal to the photon energy minus the kinetic energy of the detached electron. Thus, of two photodetachment transitions from a given anion level, the one terminating at a lower energy state of the neutral molecule appears to the right. The vertical axis represents full scale photoelectron counts. These vary considerably for different spectra, as is evident from their diverse levels of statistical noise, and range from 3000 for Cu_5^- to 20 for Cu_9^- . These differences are due to factors such as anion abundance and laser intensity, rather than to large differences in the intrinsic photodetachment cross sections.

It is apparent from the figure that the ten systems studied here all photodetach in the 0–2.4 eV (0–19 000 cm^{-1}) region accessible in this experiment.⁷¹ The positions of the intensity maxima of the lowest energy bands determine the vertical electron binding energies of the anions, except in the case of Cu_3^- , whose very weak, low energy feature is almost certainly an electronic hot band (see below). These vertical binding energies correspond to transitions from the ground electronic state of the anion to the identical (unrelaxed) geometry in the neutral molecule ground electronic state, and are listed in the first column of Table I. Arrows indicate adiabatic electron affinities, which correspond to the transition to the equilibrium geometry of the neutral molecule. The method used to obtain these values is described below.

These results display two important trends. First, there is an overall increase in electron binding energies with cluster size, from 0.9 eV for Cu_2^- to 2.0 eV for Cu_{10}^- . Superimposed on this gradual climb is a rapid alternation between the electron binding energies of consecutive odd and even clusters, with those containing odd numbers of atoms having higher energies. The equal electron binding energies of

Cu_5^- and Cu_6^- provide the sole exception to this pattern. Figure 3 shows that this odd/even alternation persists to the decamer, and recent threshold photodetachment experiments³⁸ trace it to at least Cu_{17}^- .

Several of the photoelectron spectra exhibit additional features. The Cu_2^- spectrum is the only one in which vibrational structure is resolved at our 10 meV (80 cm^{-1}) instrumental resolution. The analysis of this spectrum, discussed in Sec. III B 2 a, yields the anion bond length and vibrational frequency, and also provides a means to estimate the adiabatic electron affinities of the larger clusters despite the diffuseness of their bands. In addition, electronic structure is resolved cleanly in the spectra of Cu_4^- and Cu_6^- , and at least partially in the Cu_7^- and Cu_{10}^- spectra, yielding excited electronic state energies for the neutral clusters. A comparison among band intervals in these four spectra indicates that the energy of the lowest observed excited state of the neutral molecule decreases with respect to its ground state as the cluster grows. This convergence of energy levels is quite rapid: excited state energies decrease from 0.8 eV for Cu_4 to ~ 0.1 eV for Cu_{10} . The $\text{Cu}_2 \bar{A}$ state energy of 2.5 eV is also consistent with this trend. Energies of photoelectron-allowed excited electronic states, or corresponding lower limits based on the absence of observed transitions, are listed in the last column of Table I.

Isomers or excited electronic states of the anions can often be identified in photoelectron spectra by the presence of peaks with substantially reduced relative intensities. Such features were observed in the present study only in the case of Cu_3^- , whose spectrum is discussed further in Sec. III B 2 b. As noted below, the diffuseness of the polyatomic spectra can easily be accounted for simply on the basis of vibrational congestion. Thus, while it appears reasonable that the larger cluster anions should support bound excited

TABLE I. Cu_n^- photoelectron results.

	Vertical detachment energy (eV) ^a	Adiabatic electron affinity (eV) ^b	Bandwidth ^c (HWHM, meV)	Cu_n excited state (eV above ground state)
Cu	...	1.235 ± 0.005	4	[1.389, 3.786 ^d]
Cu_2	0.89 ± 0.01	0.842 ± 0.010	80	[2.534 ^e]
Cu_3	2.35 – 2.55	2.30 – 2.50
Cu_4	1.45 ± 0.02	1.40 ± 0.05	80	0.80 ± 0.02
Cu_5	1.97 ± 0.02	1.92 ± 0.05	90	$> 0.60^f$
Cu_6	1.97 ± 0.02	1.92 ± 0.05	90	0.31 ± 0.02
Cu_7	2.15 ± 0.02	2.10 ± 0.05	100	≥ 0.20
Cu_8	1.58 ± 0.02	1.53 ± 0.05	90	$> 1.00^f$
Cu_9	2.35 – 2.65	2.30 – 2.60
Cu_{10}	2.04 ± 0.02	1.99 ± 0.05	80	0.14 ± 0.03

^a Vertical electron binding energies correspond to intensity maxima of the lowest energy band systems in the photoelectron spectra.

^b Adiabatic electron affinities ($v' = 0 \leftarrow v''0$) are estimated to be 0.05 eV lower than the corresponding vertical binding energies, based on the similarity of band contours to that of the vibrationally resolved Cu_2^- spectrum.

^c Bandwidths (half-widths at half-maxima) were determined from least-squares fits of Gaussian line shapes to the right and central portions of the observed bands. Widths of individual vibronic transitions in the Cu_2^- spectrum are 8 meV (HWHM).

^d Energies of the excited $^2D_{5/2}(3d^9 4s^2)$ and $^2P_{1/2}^0(3d^{10} 4p)$ atomic states, respectively (Ref. 62).

^e The $\text{Cu}_2 \bar{A}$ state at 20 433 cm^{-1} (Ref. 75) falls outside our spectral region.

^f No excited states of Cu_5 or Cu_8 are observed.

electronic states or isomers, there is no evidence for significant population of such species in the present experiment.

Bandwidths in the photoelectron spectra of the molecular anions, listed in Table I, are surprisingly constant. In all cases in which the width of the transition to the neutral molecule ground state can be measured, including Cu_2^- , its value falls within the narrow range of 80–100 meV (half-width at half-maximum). Widths of excited state transitions in the Cu_4^- and Cu_6^- spectra are similar (70 and 90 meV, respectively). Since the ground electronic states of the neutral clusters studied here are expected to be bound with respect to dissociation by ~ 1 eV or more,^{16,18,22,27,29,55} excitation at 488 nm (2.540 eV) cannot, in general, access the dissociative part of the neutral cluster potential surface. Thus the observed bandwidths (which would correspond to lifetimes of $\sim 10^{-15}$ s) cannot be due to dissociation. Rather, they must reflect Franck–Condon profiles for the photodetachment transitions. The loss of resolved structure for clusters larger than the dimer is not surprising in view of the increased number of low-frequency vibrational modes in the polyatomic systems. At the measured ion vibrational temperature of 500 K, sequence bands associated with these additional low-frequency modes could quickly “fill in” the photoelectron spectrum even if only one extended vibrational progression occurred, as in Cu_2^- .

This similarity among bandwidths suggests that there is a constant offset throughout the copper cluster series between the intensity maximum and the band origin ($v' = 0 \leftarrow v'' = 0$), whose position determines the adiabatic electron affinity of the neutral molecule. This offset is determined to be 0.05 eV for Cu_2^- from the vibrational analysis in Sec. III B 2 a. Subtraction of this quantity from the measured vertical electron binding energies of the larger anions yields the adiabatic electron affinities listed in Table I. We estimate error bars of ± 50 meV for these values, to allow for uncertainties in identifying band centers and for the small variations among bandwidths. As is clear from the arrows in Fig. 3, these adiabatic electron affinities lie quite close to the peak centers. Measurements of electron affinities for Cu_3^- and Cu_9^- , whose spectra in this energy region include only a portion of the ground state transitions, are discussed separately in Secs. III B 2 b and III B 2 c.

Relative photodetachment cross sections were measured by normalizing total photoelectron count rates over the 0–2.4 eV (electron binding energy) region to the ion beam intensity, laser power and ion transit time through the laser beam ($\propto \sqrt{m}$). Measurements were obtained for each ion from two separate experiments and results agreed to within 50%. Excluding Cu_3^- and Cu_9^- , whose bands are only partially observable, cross sections for photodetachment at 458 nm are the same to within experimental error ($\sim 50\%$) for all of the copper anions studied. In addition, absolute cross sections were determined by comparison to O^- (6×10^{-18} cm²)⁷² to be $\sim 2 \times 10^{-17}$ cm² for the Cu_n^- ($n = 1-2, 4-8, \text{ and } 10$) anions.

The possibility for competition between dissociation and electron detachment is an interesting aspect of negative ion cluster photophysics. Although fragmentation products are not observed mass spectrometrically, the present experi-

ment provides two possible probes of photodissociation. The first is through the measurement of photodetachment cross sections. The results described above show that these values are relatively constant for the Cu_n^- anions ($n = 1-2, 4-8, \text{ and } 10$). For those copper cluster anions containing seven or more atoms it is known³⁸ that the principal visible light photoabsorption process is electron photodetachment, and that photofragmentation of the cluster anion is unimportant. Therefore, the constant cross sections obtained here indicate that photofragmentation is unimportant for the smaller clusters as well. The second possible probe of photofragmentation involves the spectroscopic detection of electron detachment from anionic photofragments via a sequential two-photon process, as is known to occur in O_3^- .⁷³ Most recently, we have observed the Ni^- photoelectron spectrum,⁷⁴ in addition to the more intense trimer ion signal, from a mass-selected Ni_3^- ion beam. This result indicates that sequential photodissociation ($\text{Ni}_3^- \Rightarrow \text{Ni}^- + \text{Ni}_2$) and photodetachment ($\text{Ni}^- \Rightarrow \text{Ni} + e^-$) had occurred during the brief (~ 20 ns) transit time of the ion through the laser beam. Among the Cu_n^- spectra, only that of Cu_6^- exhibited a feature that could possibly be assigned to a smaller cluster (Cu_5^-). However, this possibility was discounted by laser intensity dependence measurements, which showed a linear (rather than quadratic) power dependence for the Cu_6^- peak.

Since the mass resolution of our Wien filter is not sufficient to completely separate Cu_n^- from Cu_nO^- for the larger clusters (see Fig. 2), photoelectron spectra were obtained at various points along each mass peak to confirm that the spectra reported here do in fact originate from the bare clusters. Signals due to Cu_4O^- , Cu_6O^- , and Cu_8O^- were observed in scans at the high mass sides of the corresponding Cu_n^- peaks, and electron binding energies of 2.0 eV or less were measured for these anions. However, in no case was the Cu_nO^- spectrum identical to any of the features in the corresponding Cu_n^- spectrum. Additional photoelectron scans over the entire 0–2.4 eV region, not all shown in Fig. 3, were carried out for each ion but disclosed no additional features.

2. Specific clusters

a. Cu_2^- . The spectrum of Cu_2^- is unique among those reported here in displaying vibrational structure. An expanded portion of the experimental spectrum is shown by the solid line in Fig. 4. The strongest features in this spectrum correspond to a progression in the 265 cm⁻¹ vibration⁷⁵ of the neutral molecule, and “hot bands” due to transitions from excited levels of a ~ 210 cm⁻¹ anion vibration are observed in the low energy region. The change in peak spacings from 210 to 265 cm⁻¹ at the ~ 0.84 eV peak initially identifies it as the $v' = 0 \leftarrow v'' = 0$ transition.

This origin band assignment is confirmed by a Franck–Condon analysis whose results are shown in Fig. 4. Using the known vibrational frequency and anharmonicity in the neutral molecule, it was not possible to fit the observed photoelectron spectrum if any other peak were assigned as the origin. Best fits were obtained for an origin band position,

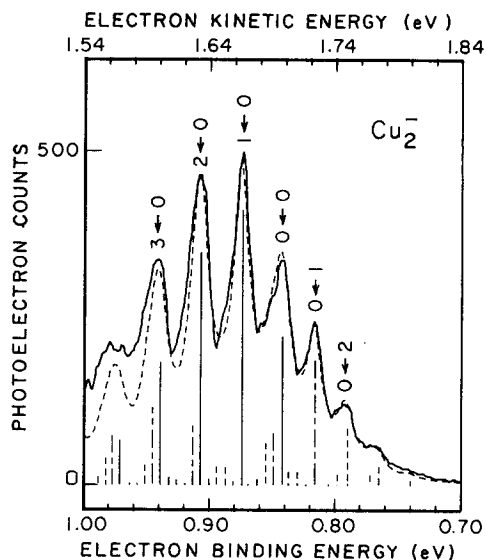


FIG. 4. Expanded 488 nm (2.540 eV) spectrum of Cu_2^- and Franck-Condon simulation (dashed contour) for $r_e' = 2.345 \text{ \AA}$, $\omega_e' = 210 \text{ cm}^{-1}$, and $T = 450 \text{ K}$. Sticks show transitions from $v'' = 0$ (solid), $v'' = 1$ (long-short dash), and $v'' = 2-4$ in the anion. Labels ($v' \leftarrow v''$) indicate the major vibronic contribution to each peak.

and thus an adiabatic electron affinity, of 0.842 eV. Consideration of energy scale calibration factors and rotational contributions suggests an error bar of 0.010 eV for this value. Assuming the anion anharmonicity equal to its value in the neutral molecule, this analysis also yields an anion frequency of $210 \pm 15 \text{ cm}^{-1}$, a temperature of $450 \pm 50 \text{ K}$, and a bond length difference of $0.125 \pm 0.010 \text{ \AA}$ with respect to the neutral molecule. This reduced ion vibrational frequency, as well as simple molecular orbital arguments, would suggest that the addition of the extra electron lengthens the bond. Thus, the neutral molecule bond length of 2.2197 \AA ⁷⁵ implies a value of $2.345 \pm 0.010 \text{ \AA}$ for the anion.

Calculated Franck-Condon factors are illustrated in Fig. 4 by solid sticks for transitions out of the anion zero point level, and by long-short and short-short dashed sticks for $v'' = 1$ and $v'' > 1$ hot bands, respectively. About equal intensities are calculated at 450 K for the $0 \leftarrow 1$ and the origin transitions, and anion levels up to $v'' = 3$ make significant contributions. The dashed simulated spectrum was generated by replacing each Franck-Condon factor stick with an 18 meV FWHM Lorentzian line shape, and shows excellent agreement with the observed spectrum up to $v' = 3$. The intensity maximum of an integrated version of the experimental spectrum would occur about midway between the $1 \leftarrow 0$ and $2 \leftarrow 0$ transitions, or about 400 cm^{-1} (50 meV) to the left of the true origin. The calculated Franck-Condon factors show that the position of this intensity maximum is not highly temperature dependent; for example, it would not be substantially shifted even for a 0 K anion.

The dissociation energy of Cu_2^- can be determined from the adiabatic electron affinities of Cu and Cu_2 and the neutral molecule bond strength ($1.96 \pm 0.06 \text{ eV}$)⁷⁶ using the relation $D_0(\text{Cu}_2^-) = D_0(\text{Cu}_2) + \text{EA}(\text{Cu}_2) - \text{EA}(\text{Cu})$. The resulting value of $D_0(\text{Cu}_2^-)$ is $1.57 \pm 0.06 \text{ eV}$, $\sim 20\%$ smaller than in the neutral molecule. A reduced anion bond

strength is qualitatively consistent with its reduced vibrational frequency, as well as with molecular orbital arguments which place the extra electron in a primarily $4s\sigma^*$ antibonding orbital. However, despite its formal bond order of only one-half, the anion bond strength considerably exceeds half the neutral molecule value.

Thus the bond strength of Cu_2^- is greater than would be expected on the basis of simple molecular orbital arguments. This phenomenon is not unique to Cu_2^- , but appears generally characteristic of metal dimer ions of either polarity. For example, comparison of the measured electron affinities⁴¹ of Fe_2 and Co_2 to the corresponding atomic values indicates that the anion bond strengths exceed those of the neutral dimers by 0.75 and 0.45 eV, respectively. The calculated bond strengths of the alkali dimer anions are comparable to the neutral molecule values, despite a formal decrease in bond order from one to one-half on electron attachment.⁷⁷⁻⁸⁰ The positive metal dimer ions exhibit a similar behavior. For example, the relative ionization potentials of Cu_2^{37} and Cu^{62} imply a Cu_2^+ bond strength that is $\sim 90\%$ of the Cu_2 value, despite a 50% loss in bond order on ionization. The dissociation energies of the $(s\sigma)^1$ alkali dimer cations are actually higher than those of the $(s\sigma)^2$ neutral molecules; for example, the K_2^+ bond strength⁸¹ exceeds that of K_2 by 50%. The measured ionization potential of Fe_2^{35} also indicates a much (1.6 eV) stronger bond in the cation. In this case, however, the increase may be due in part to a savings in atomic promotion energy,³⁵ an effect not relevant to the s^1 alkali and coinage metal systems.

These increased ion bond strengths over the values expected on the basis of bond orders alone can be accounted for, in part, by simple electrostatic considerations. The larger dimer will provide a greater stabilization of the positive or negative charge than will the atom, an effect which will increase the dissociation energy of the molecular ion. This type of effect is discussed further in Sec. IV A 1.

b. Cu_3^- . The Cu_3^- spectrum is the only one in which we detect a peak substantially weaker than the main feature. This peak, shown at a 25 times magnification in Fig. 3, is more than two orders of magnitude weaker than the higher energy feature. The photodetachment cross section for this weak feature, relative to those of the other copper cluster anions studied here, is also reduced by about a factor of 100. Thus, it is highly unlikely that this feature arises from the ground electronic state of Cu_3^- .

Two possible assignments for this peak are to a transition from an electronically excited anion, or from an impurity. Since a similar feature is observed in the spectrum of Ni_3^- , $\sim 15 \text{ amu}$ lower, such an impurity would have to be an M_2 — or M_3 — containing species. As is evident from the mass spectrum in Fig. 2, the most likely such contaminants are metal oxides. To test this possibility, we deliberately prepared copper oxides by replacing the Ar sputtering gas with O_2 . Scans at the approximate mass of Cu_3^- (mainly Cu_2O_4^-) showed no photodetachment; therefore, we conclude that the weak feature cannot be due to a copper oxide. It is also unlikely to be due to a copper cluster containing any other foreign species, since analogous features were not observed in the spectra of the other cluster anions.

Thus the best assignment for the weak band in the Cu_3^- spectrum is to an electronically excited state of the anion. We attempted to test this hypothesis by varying the flow tube length to affect the electronic temperature, but no change in relative photoelectron intensities was observed for a twofold change in tube length. This result is inconclusive, however, since the same experiments produced no change in the relative intensities of the Cu_2^- vibrational hot bands, whose assignments are secure.

With this assignment for the weak feature, the electron binding energy of Cu_3^- must be given by the relatively intense rising slope observed at high binding energy. No plateau is observed up to our cutoff at 2.35 eV; thus the vertical electron binding energy must be at least that high. An upper bound can be obtained by considering the normalized photoelectron count rate, whose value for Cu_3^- was about half the average value for the other Cu_n^- anions ($n = 1-2, 4-8, 10$). If we assume that the photodetachment cross section of Cu_3^- is not anomalous, then this count rate indicates that the most likely value of the vertical binding energy is ~ 2.4 eV. A conservative upper limit of 2.55 eV can be obtained by augmenting our 2.35 eV cutoff by about two bandwidths.

An estimate for the adiabatic electron affinity of Cu_3 of 2.30–2.50 eV is given by the 50 meV offset between adiabatic and vertical values assumed for the larger clusters. Since this offset is based on bandwidth similarities, the adiabatic value is necessarily less certain in the case of Cu_3 (and Cu_9) than for systems whose photoelectron spectra display complete peaks. Nevertheless, the measured decrease in the intensity of the Cu_3^- feature to 50% of its maximum value in 80 meV, a half-width typical for the copper cluster series, provides strong support for the present extrapolation.

On the other hand, calculations of the equilibrium geometries of the related systems Li_3^- and Ag_3^- suggest that the Cu_3^- anion may be linear. Furthermore, calculations of the neutral Cu_3 potential surface predict the linear structure to be ~ 0.2 – 0.3 eV less stable than the Jahn–Teller distorted triangular equilibrium geometry.^{13,52,54} Thus in the extreme case of a linear-to-bent photodetachment transition, the adiabatic electron affinity (for the ion and neutral equilibrium geometries) may be as much as 0.3 eV lower than the vertical electron binding energy (between linear structures). This much larger offset would imply that the electron affinity of Cu_3 could be as low as 2.0 eV. Even with these considerations, however, it is clear that the Cu_3 molecule has a very high electron affinity relative to both Cu_2 (0.842 eV) and Cu_4 (1.40 eV). This behavior mirrors its unusually low ionization potential³⁷ for formation of the (equilateral triangular) Cu_3^+ ion.

The dissociation energy of Cu_3^- into Cu^- and Cu_2 can be estimated from the relation $D_0(\text{Cu}_3^-) = D_0(\text{Cu}_3) + \text{EA}(\text{Cu}_3) - \text{EA}(\text{Cu})$. The adiabatic electron affinities (EA) in Table I and the known dissociation energy of Cu_3 ($D_0[\text{Cu}_2\text{--Cu}] = 1.08 \pm 0.19$ eV)^{2,82} then imply an energy of 2.25 ± 0.30 eV for this process. Similarly, the $\text{Cu}_3^- \Rightarrow \text{Cu} + \text{Cu}_2^-$ dissociation energy is determined to be 2.64 ± 0.30 eV. Thus the trimer bond is much stronger in the negative ion than in the neutral molecule, although the extra electron is expected to go into a nonbonding orbital in analo-

gy with the Li_3^- case. Removal of a nonbonding electron to form the positive ion also increases the bond strength. The ionization potentials of Cu ,⁶² Cu_2 ,³⁷ and Cu_3 ³⁷ imply dissociation energies of 3.0 ± 0.4 eV for $\text{Cu}_3^+ \Rightarrow \text{Cu}^+ + \text{Cu}_2$ and 3.2 ± 0.4 eV for $\text{Cu}_3^+ \Rightarrow \text{Cu}_2^+ + \text{Cu}$. As noted in the previous section, the increased ion bond strengths are due in part to the greater stability of an electron or hole when delocalized over a larger cluster.

Finally, the energy of the excited electronic state of Cu_3^- detected in these experiments can be determined with the assumption that the hot band transition accesses the ground electronic state of the neutral molecule. If this is true, then the hot band position (~ 1.5 eV) implies an energy of ~ 0.9 eV for the Cu_3^- excited state.

c. Cu_9^- . The spectrum of Cu_9^- also exhibits only a rising edge, and in this case the integrated intensity is about one-fifth that observed for the other clusters. Assuming that the electron detachment cross section and bandwidth of Cu_9^- are typical for this series, we estimate a vertical electron binding energy between 2.35 and 2.65 eV and an adiabatic electron affinity between 2.30 and 2.60 eV. The latter result is consistent with the value of 2.21–2.33 eV previously reported for the electron affinity of Cu_9 by Smalley and co-workers.³⁸

IV. DISCUSSION

A. Electron affinity vs cluster size

Experimental results now available for the copper cluster series enable some general conclusions to be drawn regarding trends in electron affinities as a function of cluster size. Adiabatic electron affinities obtained in the present work for Cu_1 – Cu_{10} are illustrated by the solid rectangles in Fig. 5. The heights of these symbols indicate uncertainties in

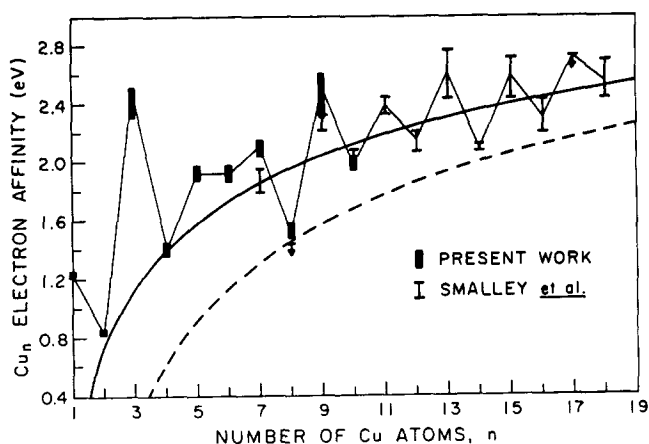


FIG. 5. Experimental electron affinities for Cu_n compared with predictions of the classical spherical drop model. Data for $n = 1$ – 10 (rectangles) are from the present work; those for $n = 7$ – 18 (bars) are from Ref. 38. Symbol sizes denote error bars except for Cu and Cu_2 , for which results are more precise than shown. Lines show electron affinities predicted by $\text{EA} = \text{WF} - 5/8(e^2/R)$, where WF is the work function of polycrystalline copper (4.65 ± 0.05 eV, Ref. 83) and R is the radius of an n -atom sphere. The dashed line shows results for $R = n^{1/3}r_b$, where $r_b = 1.41$ Å, half the average distance between atoms in the bulk. The solid line is for $R = n^{1/3}r_b + \Delta r$, where $\Delta r = a_0 (0.53$ Å).

the present measurements, except for Cu and Cu₂ for which results are more precise than indicated. Electron affinities recently reported by Smalley and co-workers,³⁸ from laser fluence dependence measurements of photoelectron signal intensities, are also shown in the figure. Although these authors were careful to emphasize that their results should be interpreted cautiously as rough estimates rather than as rigorous measurements,³⁸ we find them to be in reasonable agreement with adiabatic electron affinities determined from the photoelectron spectra. Additional laser fluence dependence measurements yielded upper bounds of 2.97 eV for the electron affinities of all clusters up to $n = 30$ except for Cu₂₉.³⁸

These data exhibit two general trends. First, there is an overall increase in electron affinities with increasing cluster size. However, for clusters up to $n = 30$, these values are still substantially lower than the work function of polycrystalline copper (4.65 ± 0.05 eV⁸³). Second, there is a clear alternation between odd and even cluster sizes, with clusters containing odd numbers of copper atoms having higher electron affinities. This oscillation is particularly pronounced at Cu₃ and Cu₈. These trends are discussed further below.

1. Approach to bulk work function: Electrostatic model

Even for a perfectly conducting cluster with a Fermi energy equal to the bulk value, electrostatic considerations show that the electron affinity (EA) will be substantially lower than the work function of the planar metal. If the cluster is modeled as a perfectly conducting sphere with radius R , then correction for the different image charge interaction than in the planar case leads^{11,20} to the prediction

$$EA = WF - \frac{5}{8} \frac{e^2}{R}, \quad (1)$$

where WF is the work function of the semi-infinite solid. For the ionization potential (IP), on the other hand, the attraction between the detached electron and the positive charge remaining on the sphere (which may be taken to reside at its center) gives rise to an additive e^2/R term^{11,20}

$$IP = WF + \frac{3}{8} \frac{e^2}{R}. \quad (2)$$

Thus as the cluster size increases, the electron affinity is expected to increase toward the bulk work function, while the ionization potential decreases (more rapidly) toward the same value. This model would predict that electron affinities for n -atom copper clusters with perfectly metallic electronic properties would still differ from the bulk work function by 1 eV at $n = 260$, and by 0.1 eV at $n = 2 \times 10^5$!

This classical "spherical drop" model has been found by Schumacher and co-workers to give remarkably good agreement with observed alkali metal cluster ionization potentials.³¹ The copper cluster series provides the first test of this model in predicting electron affinities. Application of this model to small copper clusters is physically reasonable in that these molecules are expected^{16,18,22,23,29,55} to have compact structures rather than open-chain geometries.

To apply this model to the copper cluster anions it is first necessary to evaluate R , the effective sphere radius. As a first

approximation one can take $R = n^{1/3}r_b$, where r_b is half the average distance between copper atoms in the solid. This distance, as determined from the density of bulk copper (8.93 g/cm³), is 1.41 Å. The dashed line in Fig. 5 shows the results of Eq. (1) for this choice of R . Although the calculation yields the correct general behavior, results are almost uniformly too low. The surface tension correction used by Schumacher and co-workers³¹ would reduce the value of R and decrease the calculated electron affinities still further.

A more careful consideration indicates, however, that this choice of sphere radius may not be the most physically reasonable one for small *neutral* metal clusters. In setting R to $n^{1/3}r_b$, we assume an atomic radius equal to exactly half the average internuclear distance, allowing for no orbital overlap among bonded atoms. Since the orbitals clearly do overlap, one expects the effective sphere for electron density to be shifted outward from the sphere with radius $n^{1/3}r_b$. This conclusion is supported by metal surface charge density calculations by Lang and Kohn based on the jellium model.²⁴ For parameters appropriate to copper, results show that the electron density at the surface is a considerable fraction (~40%) of the interior density.²⁴

Rather, a more appropriate form for the effective sphere radius would appear to be $R = n^{1/3}r_b + \Delta r$.⁸⁴ The additive constant Δr is analogous to the term added to each end of the chain in free electron molecular orbital models of conjugated polyenes.⁸⁵ Considering again pairs of bonded copper atoms, one can roughly estimate Δr to be in the range $1-2a_0$, where a_0 is the Bohr radius—large enough for substantial orbital overlap but less than r_b . This range is also reasonable in light of the surface density calculations mentioned above, which find that the electron density as a function of distance from the jellium surface is about halved for each increment of a_0 , reaching < 10% of the bulk density at $2a_0$.²⁴

Results of the electrostatic electron affinity calculation [Eq. (1)] for $R = n^{1/3}r_b + a_0$ are shown by the solid line in Fig. 5. As before, the work function (4.65 eV) and half the average internuclear separation (1.41 Å) are set equal to their bulk values. The calculated electron affinities are now in excellent agreement with the experimental data. The effect of the Δr term is greatest for small clusters and decreases for increasing n . Calculations for $\Delta r = 2a_0$ produce a higher, flatter curve that somewhat overestimates the electron affinities.

Thus, we conclude that the average trends observed in the electron affinities of small copper clusters are consistent with the simple electrostatic picture described above if an additive constant (in this case, a_0) is incorporated in the usual expression for the effective sphere radius. It is also interesting to note that this model predicts the electron affinities of Fe₂,⁴¹ Co₂,⁴¹ and Re₂⁴² to within 0.3 eV of their experimental values. Clearly, the effective sphere for electrons in a positively charged metal cluster will be considerably more contracted than in a neutral cluster. Thus, the Δr term should be much less important (or even of opposite sign) for ionization potentials than for electron affinities, consistent with results for the alkali cluster ionization potentials.³¹ For large n , the expressions for R used here and by Schumacher and co-workers³¹ converge to the same value.

2. Odd/even alternations and spectral line shapes

Odd > even electron affinity alternations in the copper cluster series were recently identified by Smalley and co-workers for $n = 7-17$ ³⁸ and are found to characterize the smaller clusters as well. The opposite pattern (even > odd) has been observed experimentally for the ionization potentials of Cu_n ($n = 1-7$),³⁷ Na_n ($n = 2-5$),^{32,86} and K_n ($n = 2-5$).⁸⁶ In all of these cases, the difference between values for consecutive cluster sizes is most dramatic for the trimer. The electron affinity of Cu_3 is at least 1.0 eV greater than the values for Cu_2 or Cu_4 ; analogously, the Cu_3 ionization potential is 2.1 ± 0.2 eV lower than that of Cu_2 and 1.4 ± 1.0 eV lower than that of Cu_4 .³⁷ Among metal clusters, this type of pattern has been observed or predicted^{4,8,10,12,13,16} only for the "one-electron" alkali and coinage metals. Ionization potentials of open d -shell transition metal clusters such as Nb_n ,³⁴ Fe_n ,³⁵ and Ni_n ³⁶ do not alternate.

Alternations in photoionization profiles have also been reported for neutral K_n ³³ and Cu_n ³⁷ clusters. Brechignac and Cahuzac have recently found that photoionization efficiency curves for K_n ($n = 3-8$) near threshold have linear profiles for odd n and quasiexponential profiles for even n .³³ From these single-photon results, it was inferred that Franck-Condon factors increase with vibrational quantum number in the even clusters due to a larger geometry change on electron detachment. For the copper clusters as well, Smalley and co-workers have deduced alternating shapes of photoionization curves from observed even/odd alternations in cation abundances at energies above the ionization potentials of clusters of either parity.³⁷ These results suggest that the higher ionization potentials of alkali and copper clusters containing even numbers of atoms are due to their more strongly bonding highest occupied molecular orbitals (HOMO).³⁷

In contrast to these results, the photoelectron spectra of negatively charged copper clusters display no alternations in peak shapes, although the alternations in electron affinities are more pronounced and extended than those in the alkali ionization potentials. For example, although the photoionization efficiency curves of K_5 and K_8 show clear differences,³³ we find the peak shapes of Cu_5^- and Cu_8^- to be identical. This result implies similar Franck-Condon factors for photodetachment transitions from the odd and even copper cluster anions, and suggests that the orbitals associated with the extra electrons in the anions vary less in their bonding character than do the HOMO's of the neutral clusters. This inference is consistent with the considerably greater diffuseness of the anion HOMO. For example, extended basis set CI calculations on Li_2^- by Dixon, Gole, and Jordan⁸⁰ show that the anionic $2s\sigma_u$ orbital mixes substantially with diffuse s and p functions and is twice as "large" as the $2s\sigma_g$ orbital, as measured by the ratio of their $\langle r^2 \rangle$ values. Although no calculations have been published for Cu_2^- , it is reasonable to expect that in this system the extra electron will enter a spatially extended $7s\sigma_u$ orbital comprised of diffuse s , p , and d functions⁸⁷ and exhibiting an only mildly antibonding character. In view of these considerations, the observed electron affinity alternations may be due simply to screening effects.^{4,13} Since electrons in the same orbital are screened by

each other less effectively than by the other closed shell electrons, anions with doubly occupied HOMO's (odd n) will be more stable.

Odd/even alternations in electron affinities and ionization potentials have often been inferred from intensity variations observed^{63,64,84,88} in mass spectra. Thus it is interesting to note that while our Cu_n^- mass spectrum (Fig. 2) does exhibit some intensity alternations, the intensities generally show a very poor correlation with measured electron affinities. For example, Cu_3 has one of the highest electron affinities in this series, yet the Cu_3^- mass peak is relatively weak. In addition, the electron affinities of Cu_5 and Cu_6 are about the same, although the abundances of the corresponding anions differ by almost an order of magnitude. Other factors such as differing chemical reactivities of the various cluster anions must play an important role in determining their detected abundances.

B. Excited electronic states in neutral Cu_n

Excited electronic state energies observed in the present experiment for the neutral Cu_n ($n = 4, 6, 7$, and 10) clusters provide some insight into the HOMO-LUMO (lowest unoccupied molecular orbital) energy gap as a function of cluster size. Figure 6 illustrates the results listed in Table I. Data for $n = 5, 7$, and 8 are given as lower limits based on the partial observation ($n = 7$) or absence ($n = 5, 8$) of excited state transitions in the spectra. The \tilde{A} state of Cu_2 ,⁷⁵ which falls outside our spectral region, is also included. The atomic energy shown is for the lowest transition out of the $4s$ shell ($d^{10}s^1 \Rightarrow d^{10}p^1$), in analogy with the excited state assignments discussed below. As is evident from the figure, the energies of these lowest energy (except for Cu) "photoelec-

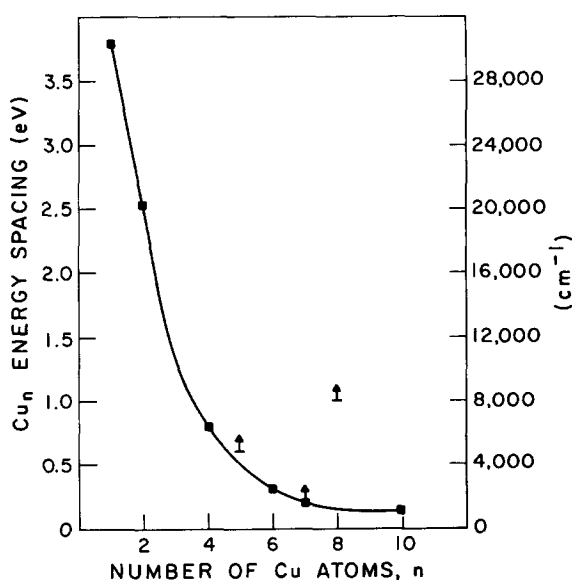


FIG. 6. Energy of the lowest observed excited electronic state in the neutral cluster (with respect to its ground state) vs the number of Cu atoms. Arrows represent lower limits based on the presence (solid square) or absence (lines) of excited state transitions in the photoelectron spectra. The energy of the lowest atomic $4s$ transition ($^2S_{1/2} \Rightarrow ^2P_{1/2}^0$) is from Ref. 62; the $\text{Cu}_2 \tilde{A}$ state energy is from Ref. 75. The 1.25 eV calculated energy for the lowest Cu_3 excited state (Ref. 52, not shown) is also consistent with this trend.

tron-allowed" excited states decrease rapidly with n . The Cu_8 cluster provides the one clear exception to this general trend.

To identify the types of electronic transitions observed, it is useful to begin with the relatively well-studied^{1,2} case of Cu_2 . The assignment of the \tilde{A} state has been a matter of some controversy, but it is probably² $^1\Sigma_u^+$.^{89,90} Excited state assignments have been given in at least five theoretical studies employing *ab initio*,^{91,92} $X\alpha$ ^{93,94} and extended Hückel²⁷ methods, and these unanimously agree that the lowest $^1\Sigma_u^+$ state arises from the $4s\sigma_g \rightarrow 4s\sigma_u^*$ transition. Since the "extra" electron in Cu_2^- also goes into the $4s\sigma_u^*$ orbital (in analogy with Li_2^- discussed above), it is clear that detachment from the $(4s\sigma_g)^2 (4s\sigma_u^*)$ anion could produce either the $(4s\sigma_g)^2 \tilde{X}$ state or the $(4s\sigma_g) (4s\sigma_u^*) \tilde{A}$ state in an allowed photodetachment process.

Assuming nondegenerate orbitals, this assignment scheme can be extended to the other even-numbered clusters. Consistent with this picture, *ab initio* calculations for small neutral copper clusters agree that the highest occupied orbitals are mainly $4s$ -like.^{18,22,23,52,92} Thus, the first excited state observed in the photoelectron spectrum should be associated with the HOMO \Rightarrow LUMO transition in the neutral cluster.

For odd clusters with nondegenerate orbitals, it might be expected that the HOMO \Rightarrow LUMO transition would not necessarily be accessible in the present experiment, since the LUMO in the neutral molecule may also be unoccupied in the anion. However, in view of the diffuseness expected for the anion orbital, such a transition would probably be observable due to orbital mixing effects. Such effects account for the strength of the $\text{Cs}^- (^1S) \Rightarrow \text{Cs} (^2P) + e^-$ photoelectron transition, for example.⁹⁵ Unfortunately, the allowed nature of such a transition is somewhat moot since the higher electron affinities of the odd copper clusters cause their lowest excited states to fall partially or completely outside our spectral region. Among the odd- n clusters, the highest quality excited state calculations⁵² have been done for Cu_3 . These SCF/CI results find the lowest excited state to result from the transition from the nonbonding, doubly degenerate $4se^1$ HOMO to a mixed valence-Rydberg type orbital. This optically forbidden $^2A_2^-$ state is predicted to occur at 1.25 eV—falling exactly on the curve in Fig. 6!

Thus, the excited state energies shown in Fig. 6 probably correspond to the lowest energy transitions involving molecular orbitals of primarily $4s$ atomic parentage. The observed trend is consistent with the expectation that the transition energy will decrease with increasing cluster size, although the result for Cu_8 indicates that this behavior need not be monotonic. The extremely rapid decrease in excited state energies with cluster size observed here ($\propto 1/n^{1.8}$) may be due primarily⁹⁶ to deviations from spherical symmetry¹² or other effects specific to these very small clusters. This high-order n -dependence cannot necessarily be extrapolated to larger particles.

The high energy (> 1.0 eV) of the lowest Cu_8 excited state suggests that its ground electronic state may have a special stability. Consistent with this notion, the electron affinity of Cu_8 is conspicuously low (see Figs. 3 and 5).

These observations are especially intriguing in view of mass spectrometric reports of intensity discontinuities at clusters containing eight alkali^{31,84} or coinage metal^{63,64} atoms. This "magic number" has been attributed by several investigators to the electronic stability of a closed-shell s^2p^6 jellium system.^{15,63,84} However, the lack of an abrupt change in alkali cluster ionization potentials at $n = 8$ was interpreted by Schumacher and co-workers³¹ as a strong argument against this model. In the neutral copper clusters, on the other hand, the present results for both electron affinities and electronic transition energies indicate a discontinuity in electronic properties at Cu_8 .

V. SUMMARY

The laser photoelectron spectra of Cu_n^- ($n = 1-10$) have been obtained at 458 and 488 nm excitation at an instrumental resolution of 10 meV. The anions were prepared in a flowing afterglow source equipped with a cold cathode dc discharge. A wide range of metal clusters can be synthesized by this method simply by varying the cathode material. Vibrational temperatures of anions extracted from the flowing afterglow source are estimated to be 500 K based on hot band intensities in the vibrationally resolved photoelectron spectra of Cu_2^- and CuF^- . This value also provides an upper limit for the rotational temperature. This very simple device is thus a general and convenient source of continuous, near-thermal beams of metal cluster anions at intensities of up to 10^{-11} A (10^8 ions/s), sufficient for spectroscopic or chemical studies. Although positive ions were not monitored in these experiments, previous reports of abundant atomic metal cation production in flowing afterglow cold cathode dc discharges^{43(a)} suggest that metal cluster cations could also readily be prepared by this method.

Electron affinities of the copper series increase with cluster size from 0.842 ± 0.010 eV for Cu_2 to 1.99 ± 0.05 eV for Cu_{10} . The overall trend in these values, and those measured by Smalley and co-workers³⁸ for larger copper clusters, has been compared with the predictions of a simple electrostatic model for the size dependence of the electron affinity of a perfectly conducting sphere. Good agreement is obtained if the effective sphere radius is taken to be $n^{1/3}r_b + a_0$, where n is the number of copper atoms and r_b is half the average bulk internuclear separation (1.41 Å). The additive constant allows for the extension of electron density beyond the positive core radius in the neutral metal cluster produced on electron detachment.

An odd $>$ even alternation in electron affinities with the number of atoms in the cluster (see also Ref. 38) is superimposed on the overall increase with cluster size. The only clear exceptions to this pattern up to Cu_{16} are the equal electron affinities of Cu_5 and Cu_6 . In contrast, the overall shapes of the photoelectron bands, which reflect Franck-Condon factors for the photodetachment process, are virtually identical in all of the cases we can measure ($n = 2, 4-8, 10$). In addition, the photodetachment cross sections of these anions at 488 nm are the same to within about a factor of 2 ($\sim 2 \times 10^{-17}$ cm²) and display no even/odd alternations. Assuming nondegenerate orbitals, the observed alternations

in electron affinities are consistent with the greater stability of closed shell anions (odd atom clusters) due to screening effects.

Excited electronic states of the neutral clusters are observed in the photoelectron spectra of Cu_4^- , Cu_6^- , Cu_7^- , and Cu_{10}^- . These states probably correspond to excitations out of molecular orbitals in the neutral clusters of primarily 4s atomic parentage. The energies of these excited states decrease rapidly with cluster size, from 0.80 ± 0.02 eV for Cu_4 to 0.14 ± 0.03 eV for Cu_{10} . The energies of the \bar{A} state of Cu_2 (2.534 eV) and the lowest excited state calculated⁵² for Cu_3 (1.25 eV) are also consistent with this trend.

Additional information was obtained concerning several of the species investigated. For Cu_2^- , vibrational structure in the photoelectron spectrum yields an anion bond length of 2.345 ± 0.010 Å and a vibrational frequency of 210 ± 15 cm^{-1} . The $\text{Cu}_2^- \Rightarrow \text{Cu}^- + \text{Cu}$ dissociation energy is determined to be 1.57 ± 0.06 eV, somewhat reduced from the 1.96 ± 0.06 eV value⁷⁶ in the neutral molecule, but larger than might be expected based on a formal reduction in bond order from one to one-half on electron attachment. The $\text{Cu}_3^- \Rightarrow \text{Cu}^- + \text{Cu}_2$ dissociation energy is 2.25 ± 0.30 eV, considerably higher than the neutral molecule value^{2,82} of 1.08 ± 0.19 eV. These increased bond strengths over the values expected on the basis of bond orders alone, which have also been observed in other positive and negative metal cluster ions, must be due at least in part to the greater stability of the extra charge when delocalized over a larger cluster. The Cu_3^- spectrum also displays a weak transition from an electronically excited state of the anion at ~ 0.9 eV. For Cu_8 , results for both electron affinities and electronic transition energies suggest that the ground state may have a special stability.

ACKNOWLEDGMENTS

We are grateful for advice and encouragement from Dr. Mike Alexander, Professor Paul Engelking, Dr. Karl Persson, Professor Art Phelps, and Mr. Richard Weppner during the development of the metal cluster ion source. This research was supported in part by the National Science Foundation under Grant Nos. CHE83-16628 and PHY86-04504 to the University of Colorado, and in part by the Donors of the Petroleum Research Fund, administered by the American Chemical Society.

¹W. Weltner, Jr. and R. J. Van Zee, *Annu. Rev. Phys. Chem.* **35**, 291 (1984).

²M. D. Morse, *Chem. Rev.* (submitted).

³D. E. Beck, *Solid State Commun.* **49**, 381 (1984).

⁴S. C. Richtsmeier, R. A. Eades, D. A. Dixon, and J. L. Gole, in *Metal Bonding and Interactions in High Temperature Systems*, edited by J. L. Gole and W. C. Stwalley, ACS Symp. Ser. 179 (American Chemical Society, Washington, D.C., 1982), p. 177; J. L. Gole, R. H. Childs, D. A. Dixon, and R. A. Eades, *J. Chem. Phys.* **72**, 6368 (1980).

⁵J. L. Martins, R. Car, and J. Buttet, *Surf. Sci.* **106**, 265 (1981).

⁶H. Basch, *J. Am. Chem. Soc.* **103**, 4657 (1981).

⁷C. F. Melius, T. H. Upton, and W. A. Goddard III, *Solid State Commun.* **28**, 501 (1978); T. H. Upton, W. A. Goddard III, and C. F. Melius, *J. Vac. Sci. Technol.* **16**, 531 (1979).

⁸R. C. Baetzold, *J. Chem. Phys.* **68**, 555 (1978); *J. Catal.* **29**, 129 (1973); *J. Chem. Phys.* **55**, 4363 (1971).

⁹M. Cini, *J. Catal.* **37**, 187 (1975).

¹⁰P. Joyes, *J. Phys. Chem. Solids* **32**, 1269 (1971).

¹¹J. M. Smith, *AIAA J.* **3**, 648 (1965).

¹²J. L. Martins, J. Buttet, and R. Car, *Phys. Rev. B* **31**, 1804 (1985).

¹³S.-W. Wang, *J. Chem. Phys.* **82**, 4633 (1985).

¹⁴W. Ekardt, *Phys. Rev. B* **29**, 1558 (1984).

¹⁵M. Y. Chou, A. Cleland, and M. L. Cohen, *Solid State Commun.* **52**, 645 (1984).

¹⁶(a) J. Flad, G. Igel-Mann, H. Preuss, and H. Stoll, *Chem. Phys.* **90**, 257 (1984); *Surf. Sci.* **156**, 379 (1985); (b) J. Flad, G. Igel, M. Dolg, H. Stoll, and H. Preuss, *Chem. Phys.* **75**, 331 (1983); (c) J. Flad, H. Stoll, and H. Preuss, *J. Chem. Phys.* **71**, 3042 (1979).

¹⁷D. R. Snider and R. S. Sorbello, *Solid State Commun.* **47**, 845 (1983).

¹⁸H. Tatewaki, E. Miyoshi, and T. Nakamura, *J. Chem. Phys.* **76**, 5073 (1982); E. Miyoshi, H. Tatewaki, and T. Nakamura, *Int. J. Quantum Chem.* **23**, 1201 (1983).

¹⁹G. Pacchioni, H.-O. Beckmann, and J. Koutecky, *Chem. Phys. Lett.* **87**, 151 (1982).

²⁰D. M. Wood, *Phys. Rev. Lett.* **46**, 749 (1981).

²¹H. Basch, M. D. Newton, and J. W. Moskowitz, *J. Chem. Phys.* **73**, 4492 (1980).

²²C. Bachmann, J. Demuyck, and A. Veillard, *Faraday Symp.* **14**, 170 (1980); J. Demuyck, M.-M. Rohmer, A. Strich, and A. Veillard, *J. Chem. Phys.* **75**, 3443 (1981).

²³R. P. Messmer, S. K. Knudson, K. H. Johnson, J. B. Diamond, and C. Y. Yang, *Phys. Rev. B* **13**, 1396 (1976); R. P. Messmer, T. C. Caves, and C. M. Kao, *Chem. Phys. Lett.* **90**, 296 (1982).

²⁴N. D. Lang and W. Kohn, *Phys. Rev. B* **1**, 4555 (1970).

²⁵R. Kubo, *J. Phys. Soc. Jpn.* **17**, 975 (1962).

²⁶R. C. Baetzold and R. E. Mack, *J. Chem. Phys.* **62**, 1513 (1975).

²⁷A. B. Anderson, *J. Chem. Phys.* **68**, 1744 (1978).

²⁸D. M. Wood and N. W. Ashcroft, *Phys. Rev. B* **25**, 6255 (1982).

²⁹B. Delley, D. E. Ellis, A. J. Freeman, E. J. Baerends, and D. Post, *Phys. Rev. B* **27**, 2132 (1983).

³⁰E. J. Robbins, R. E. Leckenby, and P. Willis, *Adv. Phys.* **16**, 739 (1967); P. J. Foster, R. E. Leckenby, and E. J. Robbins, *J. Phys. B* **2**, 478 (1969).

³¹M. M. Kappes, M. Schär, P. Radi, and E. Schumacher, *J. Chem. Phys.* **84**, 1863 (1986).

³²K. I. Peterson, P. D. Dao, R. W. Farley, and A. W. Castleman, Jr., *J. Chem. Phys.* **80**, 1780 (1984); T. D. Märk and A. W. Castleman, Jr., *Adv. At. Mol. Phys.* **20**, 92 (1985).

³³C. Brechignac and Ph. Cahuzac, *Chem. Phys. Lett.* **117**, 365 (1985).

³⁴R. L. Whetten, M. R. Zakin, D. M. Cox, D. J. Trevor, and A. Kaldor, *J. Chem. Phys.* **85**, 1697 (1986).

³⁵E. A. Rohlfing, D. M. Cox, A. Kaldor, and K. H. Johnson, *J. Chem. Phys.* **81**, 3846 (1984).

³⁶E. A. Rohlfing, D. M. Cox, and A. Kaldor, *J. Phys. Chem.* **88**, 4497 (1984).

³⁷D. E. Powers, S. G. Hansen, M. E. Geusic, D. L. Michalopoulos, and R. E. Smalley, *J. Chem. Phys.* **78**, 2866 (1983).

³⁸L.-S. Zheng, C. M. Karner, P. J. Brucat, S. H. Yang, C. L. Pettiette, M. J. Craycraft, and R. E. Smalley, *J. Chem. Phys.* **85**, 1681 (1986).

³⁹C. Brechignac, M. Broyer, Ph. Cahuzac, G. Delacretaz, P. Labastie, and L. Wöste, *Chem. Phys. Lett.* **120**, 559 (1985).

⁴⁰R. D. Mead, A. E. Stevens, and W. C. Lineberger, in *Gas Phase Ion Chemistry*, edited by M. T. Bowers (Academic, New York, 1984), Vol. III, pp. 213-248.

⁴¹D. G. Leopold and W. C. Lineberger, *J. Chem. Phys.* **85**, 51 (1986).

⁴²D. G. Leopold, T. M. Miller, and W. C. Lineberger, *J. Am. Chem. Soc.* **108**, 178 (1986).

⁴³(a) E. E. Ferguson, F. C. Fehsenfeld, and A. L. Schmeltekopf, *Adv. At. Mol. Phys.* **5**, 1 (1969); (b) V. M. Bierbaum, G. B. Ellison, and S. R. Leone, in *Gas Phase Ion Chemistry*, edited by M. T. Bowers (Academic, New York, 1984), Vol. III, pp. 1-39; (c) D. Smith and N. G. Adams, *ibid.* Vol. I (1979), pp. 1-44.

⁴⁴M. Moskovits and J. E. Hulse, *J. Chem. Phys.* **67**, 4271 (1977).

⁴⁵D. P. DiLella, K. V. Taylor, and M. Moskovits, *J. Phys. Chem.* **87**, 524 (1983); M. Moskovits, *Chem. Phys. Lett.* **118**, 111 (1985).

⁴⁶J. A. Howard, K. F. Preston, R. Sutcliffe, and B. Mile, *J. Phys. Chem.* **87**, 536 (1983).

- ⁴⁷M. D. Morse, J. B. Hopkins, P. R. R. Langridge-Smith, and R. E. Smalley, *J. Chem. Phys.* **79**, 5316 (1983).
- ⁴⁸W. H. Crumley, J. S. Hayden, and J. L. Gole, *J. Chem. Phys.* **84**, 5250 (1986).
- ⁴⁹E. A. Rohlfing and J. J. Valentini, *Chem. Phys. Lett.* **126**, 113 (1986).
- ⁵⁰D. G. Truhlar, T. C. Thompson, and C. A. Mead, *Chem. Phys. Lett.* **127**, 287 (1986).
- ⁵¹J. W. Zwanziger, R. L. Whetten, and E. R. Grant, *J. Phys. Chem.* **90**, 3298 (1986).
- ⁵²S. P. Walch and B. C. Laskowski, *J. Chem. Phys.* **84**, 2734 (1986).
- ⁵³G. H. Jeung, M. Pelissier, and J. C. Barthelat, *Chem. Phys. Lett.* **97**, 369 (1983).
- ⁵⁴S. C. Richtsmeier, J. L. Gole, and D. A. Dixon, *Proc. Natl. Acad. Sci. U.S.A.* **77**, 5611 (1980).
- ⁵⁵S. C. Richtsmeier, D. A. Dixon, and J. L. Gole, *J. Phys. Chem.* **86**, 3937 (1982).
- ⁵⁶J. A. Howard, R. Sutcliffe, J. S. Tse, and B. Mile, *Chem. Phys. Lett.* **94**, 561 (1983).
- ⁵⁷D. G. Leopold, K. K. Murray, A. E. S. Miller, and W. C. Lineberger, *J. Chem. Phys.* **83**, 4849 (1985).
- ⁵⁸S. Feigerle, Ph.D. thesis, University of Colorado, 1983 (unpublished); M. W. Siegel, R. J. Celotta, J. L. Hall, J. Levine, and R. A. Bennett, *Phys. Rev. A* **6**, 607 (1972).
- ⁵⁹J. Cooper and R. N. Zare, *J. Chem. Phys.* **48**, 942 (1968).
- ⁶⁰D. G. Leopold, T. M. Miller, and W. C. Lineberger (unpublished work).
- ⁶¹H. Hotop and W. C. Lineberger, *J. Phys. Chem. Ref. Data* **14**, 731 (1985).
- ⁶²C. E. Moore, *Natl. Bur. Stand. (U.S.) Circ. No. 467* (U.S. GPO, Washington, D.C., 1952).
- ⁶³I. Katakuse, T. Ichihara, Y. Fujita, T. Matsuo, T. Sakurai, and H. Matsuda, *Int. J. Mass Spectrom. Ion Proc.* **67**, 229 (1985).
- ⁶⁴G. Hortig and M. Müller, *Z. Phys.* **221**, 119 (1969).
- ⁶⁵N. Laegreid and G. K. Wehner, *J. Appl. Phys.* **32**, 365 (1961).
- ⁶⁶V. M. Bierbaum, G. B. Ellison, and S. R. Leone, in *Gas Phase Ion Chemistry*, edited by M. T. Bowers (Academic, New York, 1984), pp. 1–39, Vol. III.
- ⁶⁷H. Böhringer, M. Durup-Ferguson, D. W. Fahey, F. C. Fehsenfeld, and E. E. Ferguson, *J. Chem. Phys.* **79**, 4201 (1983).
- ⁶⁸G. M. McClelland, K. L. Saenger, J. J. Valentini, and D. R. Herschbach, *J. Phys. Chem.* **83**, 947 (1979).
- ⁶⁹D. G. Leopold, A. E. S. Miller, and W. C. Lineberger, *J. Am. Chem. Soc.* **108**, 1379 (1986).
- ⁷⁰T. M. Miller, D. G. Leopold, K. K. Murray, and W. C. Lineberger, *J. Chem. Phys.* **85**, 2368 (1986).
- ⁷¹Since electron detection efficiencies fall steeply for kinetic energies below ~0.3 eV, use of the 2.707 eV Ar⁺ laser line effectively extends our spectral range to 2.4 eV.
- ⁷²L. M. Branscomb, S. J. Smith, and G. Tisone, *J. Chem. Phys.* **43**, 2906 (1965).
- ⁷³S. E. Novick, P. C. Engelking, P. L. Jones, J. H. Futrell, and W. C. Lineberger, *J. Chem. Phys.* **70**, 2652 (1979).
- ⁷⁴R. R. Corderman, P. C. Engelking, and W. C. Lineberger, *J. Chem. Phys.* **70**, 4474 (1979).
- ⁷⁵K. Huber and G. Herzberg, *Molecular Spectra and Molecular Structure. IV* (Van Nostrand, New York, 1979).
- ⁷⁶K. Hilpert, *Ber. Bunsenges. Phys. Chem.* **83**, 161 (1979).
- ⁷⁷H. Partridge, D. A. Dixon, S. P. Walch, C. W. Bauschlicher, Jr., and J. L. Gole, *J. Chem. Phys.* **79**, 1859 (1983).
- ⁷⁸H. Partridge, C. W. Bauschlicher, Jr., and P. E. M. Siegbahn, *Chem. Phys. Lett.* **97**, 198 (1983).
- ⁷⁹R. Shepard, K. D. Jordan, and J. Simons, *J. Chem. Phys.* **69**, 1788 (1978).
- ⁸⁰D. A. Dixon, J. L. Gole, and K. D. Jordan, *J. Chem. Phys.* **66**, 567 (1977).
- ⁸¹M. Broyer, J. Chevalere, G. Delacretaz, S. Martin, and L. Wöste, *Chem. Phys. Lett.* **99**, 206 (1983).
- ⁸²K. Hilpert and K. A. Gingerich, *Ber. Bunsenges. Phys. Chem.* **84**, 739 (1980).
- ⁸³D. E. Eastman, *Phys. Rev. B* **2**, 1 (1970).
- ⁸⁴W. D. Knight, K. Clemenger, W. A. de Heer, W. A. Saunders, M. Y. Chou, and M. L. Cohen, *Phys. Rev. Lett.* **52**, 2141 (1984); see especially Refs. 4 and 5 therein.
- ⁸⁵I. N. Levine, *Quantum Chemistry* (Allyn and Bacon, Boston, 1983), p. 465.
- ⁸⁶A. Herrmann, E. Schumacher, and L. Wöste, *J. Chem. Phys.* **68**, 2327 (1978).
- ⁸⁷Unpublished calculations show that the Cu₂⁻ orbital associated with the extra electron does indeed have this type of complex composition (private communication from W. von Niessen).
- ⁸⁸R. E. Honig, *J. Chem. Phys.* **22**, 126 (1954).
- ⁸⁹J. Lochet, *J. Phys. B* **11**, L55 (1978).
- ⁹⁰V. E. Bondybey and J. H. English, *J. Phys. Chem.* **87**, 4647 (1983); V. E. Bondybey, *J. Chem. Phys.* **77**, 3771 (1982).
- ⁹¹M. Witko and H.-O. Beckmann, *Mol. Phys.* **47**, 945 (1982).
- ⁹²E. Miyoshi, H. Tatewaki, and T. Nakamura, *J. Chem. Phys.* **78**, 815 (1983).
- ⁹³G. A. Ozin, H. Huber, D. McIntosh, S. Mitchell, J. G. Norman, Jr., and L. Noodleman, *J. Am. Chem. Soc.* **101**, 3504 (1979).
- ⁹⁴G. S. Painter and F. W. Averill, *Phys. Rev. B* **28**, 5536 (1983).
- ⁹⁵A. Kasdan and W. C. Lineberger, *Phys. Rev. A* **10**, 1658 (1974).
- ⁹⁶R. L. Whetten (private communication).